

# A fully $(3+1)$ -D Regge calculus model of the Kasner cosmology

Adrian P. Gentle<sup>†</sup> and Warner A. Miller<sup>§</sup>

Theoretical Division (T-6, MS B288),  
Los Alamos National Laboratory, Los Alamos, NM 87545, USA.

**Abstract.** We describe the first discrete-time 4-dimensional numerical application of Regge calculus. The spacetime is represented as a complex of 4-dimensional simplices, and the geometry interior to each 4-simplex is flat Minkowski spacetime. This simplicial spacetime is constructed so as to be foliated with a one parameter family of spacelike hypersurfaces built of tetrahedra. We implement a novel two-surface initial-data prescription for Regge calculus, and provide the first fully 4-dimensional application of an implicit decoupled evolution scheme (the “Sorkin evolution scheme”). We benchmark this code on the Kasner cosmology — a cosmology which embodies generic features of the collapse of many cosmological models. We (1) reproduce the continuum solution with a fractional error in the 3-volume of  $10^{-5}$  after 10000 evolution steps, (2) demonstrate stable evolution, (3) preserve the standard deviation of spatial homogeneity to less than  $10^{-10}$  and (4) explicitly display the existence of diffeomorphism freedom in Regge calculus. We also present the second-order convergence properties of the solution to the continuum.

PACS numbers: 04.20.-q, 04.25.Dm, 04.60.Nc.

## 1. Regge calculus as an independent tool in general relativity

In this paper we describe the first fully  $(3+1)$ -dimensional application of Regge calculus [1, 2] to general relativity. We develop an initial-value prescription based on the standard York formalism, and implement a 4-stage parallel evolution algorithm. We benchmark these on the Kasner cosmological model.

We present three findings. First, that the Regge solution exhibits second-order convergence of the physical variables to the continuum Kasner solution. Secondly,

<sup>†</sup> Permanent address: Department of Mathematics, Monash University, Clayton, Victoria 3168, Australia. Email: adrian@newton.maths.monash.edu.au

<sup>§</sup> wam@lanl.gov

Regge calculus appears to have a complete diffeomorphic structure, in that we are free to specify three shift and one lapse condition per vertex. Furthermore, the four corresponding constraint equations are conserved, to within a controllable tolerance, throughout the evolution. Finally, the recently-developed decoupled parallel evolution scheme [3] (the “Sorkin evolution scheme”) yields stable evolution.

Although we have taken just the first few steps in developing a numerical Regge calculus programme, every indication (both numerical and analytic) suggests that it will be a valuable tool in the study of gravity. Our numerical studies, together with analytic results [4] should put to rest some of the recent concerns about Regge calculus [5, 6, 7] — it does appear to be a viable approximation to general relativity.

Einstein described gravitation through the curvature of a pseudo-Riemannian manifold. Regge calculus, on the other hand, describes gravity through the curvature of a piecewise flat simplicial pseudo-Riemannian manifold. The fundamental platform for Regge calculus is a lattice spacetime, wherein each lattice cell is a simplex endowed with a flat Minkowski geometry [2, 8, 9]. The physical and geometric basis of Regge calculus distinguishes it from all other discretizations of general relativity. One applies the principles of Einstein’s theory directly to the simplicial geometry in order to form the curvature, action and field equations [10]. This is in stark contrast to the finite difference approach, where one starts with a representation of the continuum field equations and proceeds to discretize them over a grid of points. The goal of our work is to evaluate the relative strengths and weaknesses of Regge calculus.

The geometrically transparent nature of Regge calculus should be useful in the interpretation of simulations. One example of this is the Kirchoff-like form of the contracted Bianchi identity [4, 11] in Regge calculus. All edges in the lattice geometry, in a strict sense, carry a flow of energy-momentum, and the sum of these flows at each vertex is zero. This single example illustrates that every term in every Regge equation has a clear geometric interpretation.

We choose to benchmark our code on the Kasner cosmology because it has a well defined solution with symmetries. More importantly, however, the Kasner model is a prototype of the Belinsky-Khalatnikov-Lifschitz mixmaster oscillation generic to all crunch cosmologies [12]. Unlike all previous Regge simulations, we impose no symmetries on the model — it is free to exhibit all dynamical degrees of freedom. The symmetries of the Kasner cosmology are encoded in the freely specifiable portion of the initial data, and the full Regge initial-value problem is then solved. The solution obtained displays encouraging agreement with the continuum Kasner solution, and this agreement is found to be remarkably well preserved during evolution. The code used in these calculations is applicable to  $S^3 \times R^1$  spacetimes, as well as the  $T^3 \times R^1$  topology presented here.

There are two major areas of active research in numerical relativity today. The first effort deals with gravitational wave generation by astrophysical processes. The

Laser Interferometric Gravity Wave Observatory, which should be operational within a few years, will require a set of gravity wave templates from colliding and coalescing black holes. The second area of research deals with the structure of cosmological singularities in inhomogeneous cosmologies. The gravity wave problem is dominated in many ways by boundary conditions, whilst the cosmological singularity problems have no boundary. We have chosen to focus our initial application of Regge calculus toward issues in inhomogeneous cosmology.

In this paper we will develop the simplicial lattice used in the calculations (section 2), and then briefly describe the geometric and dynamical structure of Regge calculus (section 3). These ideas will be applied to motivate a York-style two-surface initial-value prescription for Regge calculus (section 4), which is then specialized to the Kasner cosmology (section 5). With initial data in hand, we proceed to the time evolution problem in section 6, and apply a four-step implementation of the Sorkin evolution scheme. We examine the convergence of the Regge solution to the continuum, and confirm the existence of simplicial gauge freedoms by demonstrating that the constraint equations are satisfactorily preserved during evolution. Finally, in section 7, we discuss our future plans for numerical Regge calculus.

## 2. Kinematics and the Quantity Production Lattice

The first issue one must address when beginning a Regge calculus simulation is the choice of lattice structure. How do we choose to represent a spacetime geometry with a lattice geometry? We are aided in our decision by the following four guiding principles

- (i) We want the simplicial spacetime foliated into 3-dimensional tetrahedral spacelike hypersurfaces. Although these hypersurfaces will be geometrically distinct, their lattice structure should be identical. The spacetime sandwiched between any two of these surfaces should be decomposed into simplexes.
- (ii) Each spacelike hypersurface should have the topology of a 3-torus ( $T^3$ ).
- (iii) The simplicial structure sandwiched between two adjacent hypersurfaces must be consistent with the recently proposed Sorkin evolution scheme [3].
- (iv) The lattice connectivity, or local topology, of the 3-geometries should be maximally homogeneous. In other words, the lattice structure at one vertex should be identical to all others.

These four guiding principles have led us to the choice of lattice described below. It is in this sense that we have introduced a  $(3+1)$  split of spacetime in Regge calculus.

The fundamental geometric element in Regge calculus is the four-simplex, consisting of five vertices, ten edges, ten triangular hinges, and five tetrahedra. In this section we build the four dimensional simplicial lattice by constructing a simplicial three geometry, and then carry the triangulation of  $T^3$  forward in time, to obtain a simplicial manifold

with topology  $T^3 \times R^1$ .

The best tetrahedral subdivision of  $T^3$  that we know is based on isosceles tetrahedra, and will be referred to as the Quantity Production Lattice (QPL) [13]. A major advantage of this lattice is that it is easily refined whilst maintaining local homogeneity, in the sense that the connectivity at each vertex is the same. The QPL consists of isosceles tetrahedra only in flat Euclidean space, with slight variations in the edge lengths introducing curvature about edges in the three-lattice.

The  $T^3$  QPL may be constructed from a single cube. Begin by identifying opposing faces, thus fixing the global topology. Subdivide the cube into smaller cubes, until the desired resolution is obtained, and then introduce a new vertex at the centre of each small cube. Joining these centred vertices together yields a new cubic lattice which pierces the faces of the original. Finally, join the centred vertices to each of the eight vertices of the original cube in which they reside, creating four tetrahedra through each face of the original cubic lattice. This completes the construction of the QPL. Figure 1 displays some of the local structure of the resulting lattice.

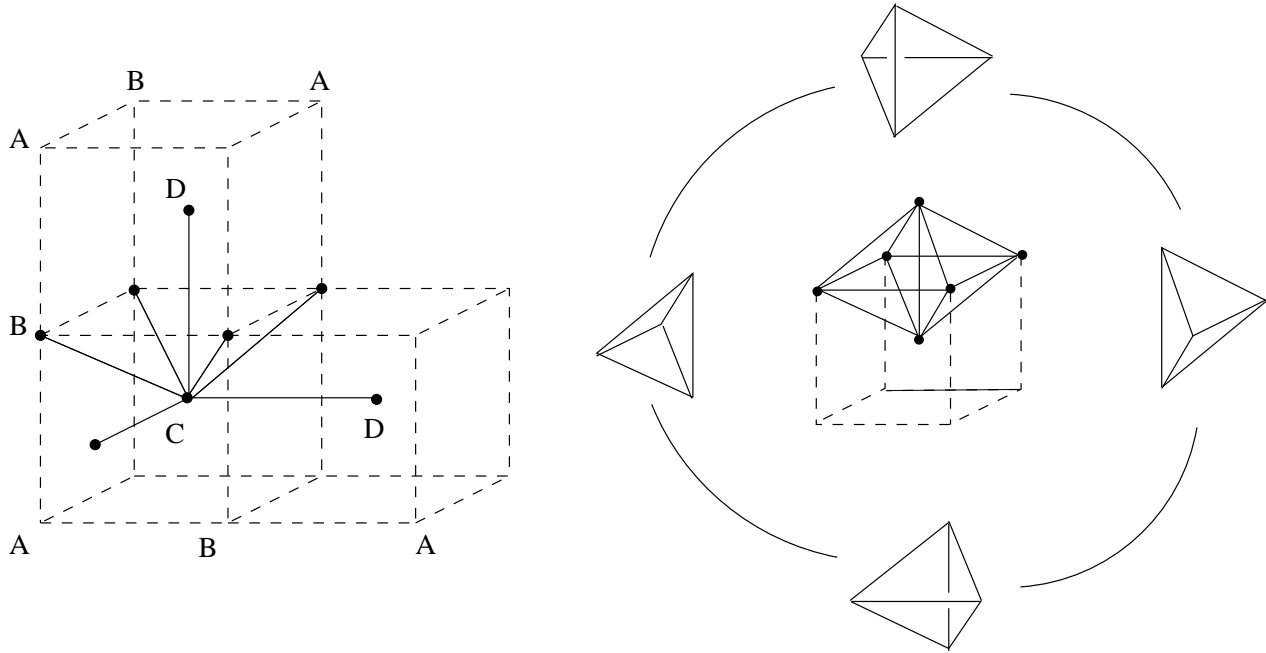


**Figure 1.** Two different views of the Quantity Production Lattice. a) The vertex data structure, which when carried from vertex to vertex generates the three-geometry. Several A-, B-, C-, and D-type vertices are also shown, and these are defined in the text below. b) The local lattice structure about a single leg. The four tetrahedra piercing a single face of the original cubic lattice are shown “exploded off”.

Fourteen edges emanate from each and every vertex in the QPL. Six legs lie along cube edges, and 8 diagonal edges join the two cubic lattices together. These two types of edges will be referred to as cube-aligned and diagonal edges, respectively. The QPL, as outlined here, is isomorphic to the right-tetrahedral lattice, which can be formed by adding face and body diagonals to a cubic grid. Despite this, we have found that assigning edge lengths using the right tetrahedral approach leads to minor numerical difficulties, due to degeneracy in the first derivatives of the Regge equations. This has perhaps impeded previous work with  $(3 + 1)$  formulations of Regge calculus [14].

We now have in hand the simplicial three geometry, and turn to the construction of the four geometry in which this initial slice is to be embedded. The four geometry is constructed by dragging vertices forward, one by one, until the whole initial surface has been replicated, and the intervening region filled with four-simplices. We refer to the resulting lattice as a Sorkin triangulation [15, 16].

Another useful approach to the construction of the four geometry is the “vertex data structure”, whereby each vertex in the lattice has, in so far as is possible, an identical local structure. In general, the Sorkin approach to the evolution problem is inconsistent with such a lattice. The major advantage of Sorkin triangulations over a four geometry built using a vertex data structure is that it allows the use of an order  $N_v$  (number of vertices in each three-geometry), parallel, four-step evolution algorithm. That is, one quarter of the vertices in the three-geometry may be evolved together, in parallel.

We construct the Sorkin triangulation as follows. Identify four classes of vertices in the QPL, two types on the original cubic structure, and the remaining two on the cube-centred lattice. The vertex types are defined as

*A-type:* Half the vertices on the original cubic lattice, sharing no common edges.

*B-type:* The remaining vertices on the original cubic lattice.

*C-type:* Half the vertices on the cube-centred lattice, not sharing common edges.

*D-type:* Remaining vertices on the cube-centred lattice.

These identifications are indicated in figure 1. We now construct the four geometry from the simplicial three geometry.

Begin by selecting a single A-type vertex,  $A_k$  say, and drag it forward in time, to create a new vertex  $A_k^+$ . In the process we introduce 14 brace edges over the 14 legs emanating from  $A_k$  in the  $l^{th}$  spacelike hypersurface ( $\Sigma_l$ ), together with a vertical (timelike) leg joining  $A_k$  to  $A_k^+$ . This timelike edge is taken small enough to ensure that the brace edges are spacelike. Each brace edge joins the newly evolved vertex  $A_k^+$  to the corresponding vertices in the previous slice which share an edge with  $A_k$ . Figure 2 shows the situation in  $(1 + 1)$  dimensions. From the figure it is clear that “evolving” an A-type vertex creates a 2-simplex (triangle) over each 1-simplex (edge) meeting at  $A_k$ . In  $(3 + 1)$  dimensions, the procedure creates a 4-simplex above each tetrahedron

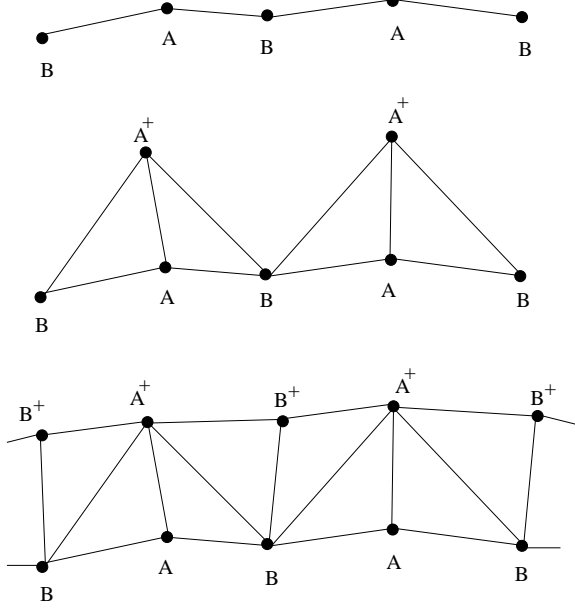


**Figure 2.** The  $(1+1)$ -dimensional analogue of the Sorkin scheme, applied to a region of the lattice. a) On the initial hypersurface, we identify A- and B-type vertices, the only requirement being that no two vertices of a given type share an edge. In  $(3+1)$  dimensions, the lattice breaks into four classes of vertices under this requirement. b) All A-type vertices are carried forward together, creating  $(n+1)$ -simplices “above” each  $n$ -simplex in the initial slice. c) The B-type vertices are dragged forward. This completes the  $(1+1)$ -D evolution procedure, replicating the original hypersurface and triangulating the intervening region.

(3-simplex) which shares the vertex  $A_k$ . Having identified the 4-simplices in this way, we may tabulate the new tetrahedra and triangles which they contain. This process can be repeated on all A-type vertices simultaneously, since none of these vertices share a common edge.

Now consider a single B-type vertex. Dragging it forward yields 8 brace legs between slices, one over each of the 8 diagonal legs in  $\Sigma_l$ . The original vertex is also joined to 6 A-type vertices which have already been dragged forward, so joining the new vertex to these creates 6 spatial legs on  $\Sigma_{l+1}$ . A vertical edge joining the new vertex to its counterpart on the original slice is also created. Again, all B-type vertices can be dragged forward in parallel, and this process creates a set of 4-simplices in a manner similar to the A-type evolution step.

Next the cube-centred C-type vertices. Each of these creates 6 brace legs between slices, since each C-type vertex in  $\Sigma_l$  is connected to 6 D-type vertices, which have yet to be carried forward. Also created are 8 spatial diagonal legs on  $\Sigma_{l+1}$ , joining the C-type to surrounding A- and B-type vertices, together with a single timelike edge. Finally,

the D-type vertices are dragged forward, creating 14 new spatial legs on  $\Sigma_{l+1}$ , together with a single timelike leg.

In this way the initial surface is carried forward in time, constructing an identical three geometry on  $\Sigma_{l+1}$ , and filling the intervening region with four-simplices. The resulting (3 + 1) Regge spacetime is consistent with our four guiding principles.

### 3. Dynamical structure of Regge calculus

In section 2 we developed the kinematic structure of the simplicial spacetime. We now apply the Regge form of Einstein's field equations to the lattice.

Regge [1, 10] constructed the simplicial form of the Hilbert action, and obtained what have become known as the Regge equations via a variational principle. The independent variables in this approach are the lattice legs. Each edge in the lattice has associated with it a simplicial equivalent of the Einstein equations, which take the form [1, 4]

$$\frac{2L}{V_L^*} \sum_h \epsilon_h \frac{\partial A_h}{\partial l_j^2} = 0, \quad (1)$$

where the summation is over all triangles  $h$  which hinge on the leg  $l_j$ . The defect  $\epsilon_h$  about  $h$  is the angle that a vector rotates when parallel transported around the hinge,  $A_h$  is the area of the hinge, and  $V_L^*$  is the 3-volume of the Voronoi cell dual to edge  $L$ . Equation 1 is the Regge calculus analogue of  $G_{\mu\nu} = 0$ .

When applied to our lattice, there are three types of Regge equation, depending on the type of edge in the lattice it is associated with. The equations associated with edges in a spacelike hypersurface may be viewed as “evolution”-type equations, since they couple information on that surface to the edges lying above and below. This is the Regge equivalent of the second order evolution equations in the ADM (3 + 1) split [9].

Equations associated with brace edges, those lying between successive spacelike hypersurfaces, only involve quantities on and between the two slices. In this sense they are “constraint” or first order equations. Similarly, the “timelike Regge equations” obtained by varying the vertical edges between two spacelike hypersurfaces are first order equations.

The Einstein tensor in the continuum is a rank 2 symmetric tensor, and hence has two indices. E. Cartan has provided us with a geometric interpretation of this tensor and its components. He showed that the Einstein tensor is expressible as a double dual of the sum of moments of rotation [9] over the 2-dimensional faces of a 3-volume. Thus one index can be interpreted as the orientation of that 3-volume, and the other can be associated with the orientation of the dual of the sum of moments of rotation.

The Cartan approach provides a derivation of the Einstein equations independent of the action, and has been successfully applied to Regge calculus [4]. The usual Regge equations are recovered as a sum of moments of rotations. Thus for each edge

$L$  in the Regge spacetime the voronoi 3-volume  $V_L^*$  dual to the edge, and each of the moment of rotation vectors over the 2-dimensional faces of  $V_L^*$  are parallel and directed along  $L$ , yielding a single Regge equation per edge. It is in this sense that the Regge equation is the double projection of the Einstein tensor along edge  $L$  (ie:  $G_{LL}$ ). Since the timelike edges in our Kasner simulation are orthogonal to the homogeneous spacelike hypersurfaces, the Regge equations associated with these edges (the “timelike Regge equations”) are the canonical Hamiltonian constraint equations. Similarly, the other first-order Regge equations, associated with the brace edges, are the only Regge equations that carry components of the momentum constraints ( $G_{0i}$ ). Thus we use three of these brace equations per vertex as momentum constraints, and the timelike Regge equation as the Hamiltonian constraint.

In continuum general relativity, the ten Einstein equations are functions of the ten components of the metric tensor. However, of these ten metric components, only six functions per spacetime point may be considered truly independent, since we have the freedom to choose a system of co-ordinates. Correspondingly, there are four relations per point amongst the Einstein equations themselves, the contracted Bianchi identities [9].

A similar structure is found in Regge geometrodynamics. Each vertex in the lattice may be associated with a unique set of  $N$  edges, and each of these edges has a corresponding Regge equation. However, the simplicial form of the contracted Bianchi identity holds at each vertex [11], a total of four constraints per vertex. So there can only be  $N - 4$  truly independent edges per vertex, with the remaining four edges representing simplicial gauge freedom. This corresponds to the lapse and shift freedom in continuum  $(3 + 1)$  relativity [9]. The four redundant Regge equations per vertex introduced in this process may be compared with the four constraint equations in continuum  $(3 + 1)$  general relativity.

The finite rotations involved in the simplicial contracted Bianchi identity do not commute, so these “identities” are only approximate [4]. In the infinitesimal limit, however, it is expected that the Regge Bianchi identities become exact in correspondence to the continuum. This failure to precisely conserve the constraints is no worse than the failure of a finite difference scheme to exactly conserve the numerical constraints. We demonstrate this conservation of energy-momentum in section 6.

#### 4. A York-type initial-value prescription for Regge calculus

Before evolution can proceed, we must construct initial data consistent with the Regge constraint equations. All previous initial data constructed in Regge calculus has been for the special case of a moment of time symmetry, where the problem reduces to the requirement that the scalar curvature of the initial three geometry is zero [8]. Successful

time-symmetric Regge calculations include initial data for single and multiple black holes [17, 18], Friedmann-Robertson-Walker and Taub cosmologies [19, 20, 21], and Brill waves on both flat [22] and black hole [23] backgrounds.

The major simplification of calculating initial data at a moment of time symmetry is that the problem reduces to the calculation of the purely three-dimensional scalar curvature, and does not involve the four dimensional lattice structure [8]. In spacetimes of astrophysical interest there will not ordinarily be a moment of time symmetry to simplify the initial-value problem. Indeed, this is the case in the Kasner class of cosmologies considered here. The discrete time Regge lattice necessitates the construction of fully four-dimensional, two-slice initial data (a “thin sandwich approach”). We apply a novel two-slice initial-value formalism, to be described in more detail elsewhere [24], to construct initial data for the Kasner cosmology in Regge calculus.

The two-surface approach outlined below is constructed to mirror, in as far as possible, the York [9, 25] technique for constructing initial data in the continuum, rather than the Belasco-Ohanian [26] two-surface formulation. The advantage of the York approach is that it clearly delineates the true degrees of freedom of the gravitational field from the embedding quantities. York begins by conformally decomposing the three-metric,

$${}^{(3)}g_{ij} = \psi^4 {}^{(3)}\tilde{g}_{ij},$$

introducing the conformal factor  $\psi$ , and base metric  $\tilde{g}_{\mu\nu}$ . We are then free to specify [9] the

- base metric  ${}^{(3)}\tilde{g}_{ij}$  (“Where”).
- momenta  $\tilde{\pi}_{ij}^{TT}$  (“How Fast”), and
- The trace of the extrinsic curvature,  $\text{Tr}K$  (“When”).

Once these have been fixed, the only remaining variables are the conformal factor  $\psi$ , and the gravitomagnetic three-vector potential  $W^i$ . The four constraint equations are used to calculate these quantities.

The key to our simplicial two-surface formulation of York’s procedure is the simplicial representation of the dynamical degrees of freedom and embedding variables. The identification presented below is by no means unique. In other words, we provide a representation of the degrees of freedom and not a diffeomorphically invariant, conformally invariant representation of the dynamic degrees of freedom. To this end, it is convenient to perform a conformal decomposition on each hypersurface, yielding leg lengths in  $\Sigma_k$  ( $k = 0, 1$ ) of the form

$$l_{ij} = \psi_{ij}^2 \tilde{l}_{ij}$$

where  $\tilde{l}_{ij}$  is the base leg between vertices  $i$  and  $j$  lying in one hypersurface, the simplicial equivalent of the base metric  ${}^{(3)}\tilde{g}_{ij}$ . The conformal factor is defined on the vertices of

the 3-lattice  $\Sigma$ , and is applied to the edge between vertices  $i$  and  $j$  using a centred, second order, approximation

$$\psi_{ij} = \frac{1}{2} (\psi_i + \psi_j).$$

Within each hypersurface, 14 edges emanate from each vertex; 6 cube-aligned, together with 8 diagonal legs. It is convenient at this stage to view the lattice, and the three-lattice in particular, from the viewpoint of a vertex data structure. The three geometry can be constructed by applying the generator shown in figure 1 to each vertex, which consists of 3 cube-aligned legs, together with 4 diagonal edges. The four geometry sandwiched between the two hypersurfaces contains a single brace leg over each of these 7 edges per vertex, and so a similar decomposition into edges per vertex can be obtained for the brace legs. However, the exact structure of these braces depends on the choice made in the construction of the four lattice, and in particular, each type of vertex (A,B,C,D) will have a different arrangement of braces about it.

Since we are dealing with a full four-dimensional region of the lattice, the initial-value problem requires that we specify lapse and shift, otherwise we would be unable to construct the thin-sandwich analogue of  $\text{Tr}K$  and  $\tilde{\pi}_{ij}^{TT}$ . These quantities both depend on derivatives of the 3-metric, the lapse function and the shift vector. Our freedom to freely choose lapse and shift is linked to the simplicial contracted Bianchi identities, discussed above [4]. Although Regge calculus deals directly with geometric, co-ordinate independent quantities, we must still specify how vertices on the initial three geometry are pushed forward in time.

The York prescription outlined above allows us to freely specify the base three-geometry (the “where” [25]),  $\text{Tr}K$  (“when”), and the momentum conjugate to the true dynamical degrees of freedom of the gravitational field (“how fast”).

A two-surface formulation of these ideas requires that the momenta terms be split across both surfaces. In direct analogy to the assignment of the base three-metric, we specify freely all base legs on the initial hypersurface  $\Sigma_0$ . To avoid specifying everything on either surface (and thus obtaining a Belasco-Ohanian style initial data prescription [26]), we must not specify the conformal factor  $\psi$  on  $\Sigma_0$ . The conformal factor at each vertex on  $\Sigma_1$  is freely specified instead, in analogy to the fixing of  $\text{Tr}K$ . The final step is to identify the Regge analogue of  $\tilde{\pi}_{ij}^{TT}$ . We choose the 4 diagonal base legs per vertex on  $\Sigma_1$  to represent this freedom, since, together with the lapse and shift choice, they enable us to specify part of the change in the base “metric” across the sandwich.

Our two-surface formulation on the lattice, in the spirit of the standard York decomposition, may be summarized as follows. Specify

- All 7 base edges  $\tilde{l}_{ij}$  per vertex on  $\Sigma_0$  (“Where”),
- The 4 diagonal base edges per vertex on  $\Sigma_1$  (“How Fast”),
- The conformal factor  $\psi_{ij}$  at each vertex on  $\Sigma_1$  (“When”), and

- 4 lapse and shift conditions per vertex (“How Fast” and “When”),

which leaves the conformal factor  $\psi$  on  $\Sigma_0$ , the 3 spatial cube-aligned edges per vertex on  $\Sigma_1$ , and the 4 braces per vertex which lie over diagonal edges as the true representations of the geometric degrees of freedom. These 8 unknowns per vertex may be calculated by solving the 8 Regge constraint equations per vertex which are available during the solution of the initial-value problem. The constraints are associated with the 7 braces per vertex, together with the timelike edge joining the vertex on  $\Sigma_0$  to its counterpart on  $\Sigma_1$ .

It is possible to introduce sophisticated definitions of lapse and shift by mirroring the continuum structure [3], however a more natural approach is to select appropriate legs in the lattice, and define them to represent the simplicial gauge freedom. In this spirit, we define lapse to be the proper time measured along a timelike leg joining a vertex to its counterpart on the next hypersurface, and the shift to be a combination of three legs that uniquely fix the location of the new vertex above the previous hypersurface.

Detailed definitions of shift differ as to which type of vertex (A,B,C or D) we are considering. The evolution of an A-type vertex creates 14 brace edges stretching between  $\Sigma_l$  and the nascent hypersurface  $\Sigma_{l+1}$ , together with a timelike “Regge lapse” edge. Six of these edges will lie above cube-aligned edges in  $\Sigma_l$ , and it is these braces that we select as our simplicial shift freedom. In particular, at a given A-type vertex, the shift edges correspond to the brace legs above the 3 cube-aligned edges in the vertex generator shown in figure 1. This definition of shift is also applied to the C-type vertices.

In the case of B- and D-type vertices, assigning the lengths of these braces will not determine the position of the evolved vertex. This can be seen in figure 2, where assigning all brace lengths will only rigidify the “A”-type vertices, leaving the “B”-type to flap. This would result in an ill-conditioned system of equations, since the location of the B-type vertices is completely undetermined. This  $(1 + 1)$ -dimensional example suggests that we define the shift edges on B- and D-type vertices by assigning the lengths of the 3 cube-aligned edges in  $\Sigma_{l+1}$ . The three edges chosen are always those associated with the vertex-by-vertex generator shown in figure 1. It is clear from this discussion that care must be taken in choosing the simplicial counterparts of lapse and shift.

## 5. Thin-sandwich initial-value approach applied to the Kasner cosmology

We now apply the initial-value formalism outlined above to the Kasner class of cosmologies. The metric for these  $T^3 \times R^1$  vacuum solutions of Einstein’s equations takes the form

$$ds^2 = -dt^2 + t^{2p_1}dx^2 + t^{2p_2}dy^2 + t^{2p_3}dz^2 \quad (2)$$

where the unknown constants  $p_i$  satisfy

$$p_1 + p_2 + p_3 = p_1^2 + p_2^2 + p_3^2 = 1. \quad (3)$$

We construct the two surface initial data such that the initial surface,  $\Sigma_0$ , is at  $t = 1$ , and  $\Sigma_1$  is at  $t = 1 + \Delta t$ . The base leg lengths on  $\Sigma_0$  are assigned the flat-space values obtained by setting  $t = 1$  in (2). This yields

$$\tilde{l}_{x_k} = \Delta x_k \quad (4)$$

for the three cube-aligned base edges per vertex on  $\Sigma_0$ , and

$$\tilde{l}_{ij}^2 = \frac{1}{4} (\Delta x^2 + \Delta y^2 + \Delta z^2). \quad (5)$$

for the 4 diagonal base edges per vertex.

The conformal factor on  $\Sigma_1$  is the simplicial equivalent of setting  $\text{Tr} K$ , and we choose to take

$$\psi = 1 \quad \text{on } \Sigma_1. \quad (6)$$

The kinematic degrees of freedom correspond to the 4 diagonal legs per vertex on  $\Sigma_1$ , and these are set in the same manner as the base diagonal legs on the initial slice, using (2) evaluated at  $t = 1 + \Delta t$ . This yields

$$\tilde{l}_{ij}^2 = \frac{1}{4} (t^{2p_1} \Delta x^2 + t^{2p_2} \Delta y^2 + t^{2p_3} \Delta z^2). \quad (7)$$

The only edges which remain to be fixed are our choice of shift and lapse. The lapse edge is assigned the squared proper time between slices,

$$\tau_{ii+}^2 = -\Delta t^2, \quad (8)$$

and the squared lengths of the shift edges are obtained by applying a power series expansion along the continuum geodesics. Accurate to third order in the lattice spacing, the expansion between vertices  $i$  and  $j$  is

$$l_{ij}^2 = g_{\mu\nu} \Delta x_{ij}^\mu \Delta x_{ij}^\nu + g_{\alpha\beta} \Gamma_{\mu\nu}^\beta \Delta x_{ij}^\alpha \Delta x_{ij}^\mu \Delta x_{ij}^\nu + \dots \quad (9)$$

where the continuum metric  $g_{\mu\nu}$  is used to obtain  $\Gamma_{\mu\nu}^\beta$ . The spatial edge length assignments above are identical to the expressions obtained from (9), to third order. In principle we could ignore the cubic term in the expansion, and take the squared shift edge lengths to be

$$l_{ij}^2 = g_{\mu\nu} \Delta x_{ij}^\mu \Delta x_{ij}^\nu, \quad (10)$$

however it was found that the initial-value problem converged faster using the higher order expansion. The simplest approximation was tested, and found not to change the character of the initial-value solution appreciably. These expansions are used only whilst

constructing initial-value data, and only when we wish to compare with a continuum metric.

The shift conditions on A- and C-type vertices are applied to brace legs lying above cube-aligned edges, and the geodesic-length approximation (9) for these yields

$$d_{x_k}^2 = -\Delta t^2 + \Delta x_k^2 + p_k \Delta x_k^2 \Delta t. \quad (11)$$

For the B- and D-type vertices, shift is applied to the three cube-aligned base spatial edges per vertex in  $\Sigma_1$ , where the series expansion takes the form

$$\tilde{l}_{x_k}^2 = -\Delta t^2 + (1 + \Delta t)^{2p_k} \Delta x_k^2. \quad (12)$$

In all calculations shown in this paper, we use the QPL obtained by two barycentric subdivisions of the original cube. The three geometry consists of 128 vertices, 896 legs, 1536 triangles and 768 tetrahedra per spatial hypersurface. The region contained between two consecutive spacelike hypersurfaces contains 3072 four-simplices. Whilst this is a modest grid resolution by modern standards, the major aim of this work is the evaluation of Regge calculus as a competitive technique in (3 + 1) numerical relativity; we feel that the grid is sufficient for this task, and experiments with increased spatial resolution do not effect the conclusions reached below.

The Kasner exponents  $p_i$  enter into the freely specifiable portion of the initial data through equations (7), (11) and (12). They are not used at any other stage of the calculations, and in particular, do not appear in the evolution problem. The information borrowed from the continuum solution in this way could, in principle, be constructed within the Regge framework by seeking a solution with the required symmetries. Analytic calculations in which the Regge lattice is forced to maintain the symmetries of the Kasner solution have been undertaken [27, 28]. These confirm that the Regge equations produce the expected Einstein equations for the Kasner cosmology to leading order in the limit of very fine discretizations. Any calculation must begin with a suitable ansatz to determine the desired class of solutions; we have chosen the freely specifiable portion of the initial data to closely model the Kasner cosmology, allowing us to compare with the analytic solution. This provides a test-bed for (3 + 1) Regge calculus, whilst maintaining maximal freedom in the non-specifiable portion of the initial data.

The spatial length scales which appear in the geodesic expansions above must be chosen for a particular simulation, noting that the total volume of the initial base geometry will be  $64\Delta x \Delta y \Delta z$ . To avoid problems with the Courant condition, the timestep is scaled together with the spatial resolution. We choose

$$\Delta t = \min\{\Delta x, \Delta y, \Delta z\} \times \Delta t_0, \quad (13)$$

where  $\Delta t_0 < 0.5$ . The only constraint on the choice of spatial length scale is the condition that we require many grid zones across the co-ordinate horizon, which for the

metric (2) is located at  $t$ , so at  $t = 1$  we require  $\Delta x_i \ll 1$  [29].

The initial-value algorithm outlined in section 4 can now be applied to the QPL model of the Kasner cosmology. The freely specifiable variables are fixed using equations (4)-(8), with equations (11) and (12) being used to enforce the shift conditions. The remaining variables at each vertex, namely the conformal factor on  $\Sigma_0$ , the four diagonal brace edges between slices, and the three cube aligned edges in  $\Sigma_1$ , are calculated by solving the available Regge equations. The resulting system of eight equations per vertex (a total of 1024 variables for the QPL considered here) is solved using Newton-Raphson iteration.

Finally, we present a sample initial data solution for an axisymmetric Kasner cosmology ( $p_1 = p_2 = 2/3, p_3 = -1/3$ ), where we take  $\Delta x = \Delta y = \Delta z = 0.005$  and  $\Delta t = 0.001$ . The initial-value solution is found to be homogeneous to a very high degree. Solving the constraints for the independent variables in this case yields the mean values

$$\begin{aligned} \psi^2 &= 1.0000000001 \\ \tilde{l}_x^2 &= 0.0000250333 \\ \tilde{l}_y^2 &= 0.0000250333 \\ \tilde{l}_z^2 &= 0.0000249833 \\ d^2 &= 0.0000177563 \end{aligned} \tag{14}$$

where  $l_x, l_y$  and  $l_z$  are the three cube-aligned legs in  $\Sigma_1$ ,  $d$  is a diagonal brace edge between slices, and  $\psi$  is the conformal factor on  $\Sigma_0$ . The standard deviation of both the edges and the conformal factor from these mean values is of the order  $10^{-10}$ , which is the convergence tolerance used for the Newton-Raphson iteration.

## 6. Time evolution of the Kasner cosmology

In the previous sections we described the structure of the quantity production lattice, and built two-surface initial data for the Kasner cosmology. We now consider the evolution of this data.

The initial data is evolved using the parallel Sorkin evolution scheme described by Barrett *et al* [3]. In section 2 we constructed the simplicial lattice from the initial 3-geometry by dragging forward individual vertices. This procedure was used because it results in a lattice suited to Sorkin evolution. The key realization in the Sorkin approach [16], based on the original examples [15], is that when a vertex is carried forward to the next slice, a new Regge equation becomes available below every new edge created. Thus a purely local evolution algorithm is possible. The evolution of a single vertex in the quantity production lattice creates 15 new edges, and makes available 15 Regge equations.

In the case of the A-type vertices, 14 brace edges are created between  $\Sigma_l$  and  $\Sigma_{l+1}$ , together with the timelike edge. This completely encloses the region surrounding the 14 spatial edges emanating from the vertex in  $\Sigma_l$ , and the timelike edge joining the vertex to its future counterpart. The Regge equations associated with the legs in  $\Sigma_l$  emanating from the vertex A, together with the timelike edge, may be used to solve for the lengths of the 14 new brace edges and single new timelike edge. A similar situation applies for the B-type vertices, except here there are 6 new cube-aligned edges in  $\Sigma_{l+1}$ , 8 new spacelike diagonal braces and a timelike leg between the Cauchy slices. In this case, the new Regge equations which become available are associated with the timelike edge, the 6 cube-aligned braces below the new spatial edge, and the 8 spatial diagonal edges in  $\Sigma_l$ . Evolving a C-type vertex creates 6 new brace edges, together with 8 spatial edges and a single timelike edge, and the available Regge equations correspond to the 6 spatial edges in  $\Sigma_0$ , 8 brace edges, and the timelike edge. Finally, D-type vertices create a vertical edge and 14 new spatial edges on the newly formed spacelike hypersurface. The evolution equations in this case are associated with the brace edges between slices and the timelike edge at the vertex.

However, this is not the entire story. As we saw in section 3, the simplicial form of the contracted Bianchi identities imply that four equations per vertex are dependent on the remaining equations. The quantity production lattice has a total of 15 dynamical edges per vertex during evolution, but we can only consider 11 of those as independent, with the remaining four freely specifiable – the simplicial equivalents of shift and lapse freedom.

We choose to apply the lapse and shift conditions on the same combination of edges as in the initial-value problem, however the technique is slightly different. Consider an A-type vertex. About this vertex there are 6 brace edges, lying above the cube-aligned edges in the current hypersurface. The zero shift condition is applied by demanding that opposing brace edges, lying along the same “axis”, have equal lengths. This condition is applied to each of the three pairs of such edges. Provided that the homogeneity of the initial slice is maintained, this ensures that the timelike edge is locally orthogonal to the current hypersurface. Similar conditions are used for the remaining vertices, applied either to brace edges (C-type) or spatial edges on the next hypersurface (B- and D-type vertices). The lapse freedom is utilised to specify the squared length of the timelike edge at each vertex.

The application of four gauge conditions per vertex leaves 11 dynamical edges and 15 equations at each vertex in the lattice. Clearly 4 Regge equations per vertex are redundant, becoming constraints which may be tracked during evolution. The redundant equation associated with lapse freedom is our “Hamiltonian constraint”, the timelike Regge equation. When applying shift conditions, we choose the redundant equation to lie below the edges upon which the gauge condition is applied. For A- and C-

type vertices, shift is applied to brace edges, so the 3 redundant equations per vertex correspond to the cube-aligned spatial edges in the vertex generator (see figure 1). For B- and D-type vertices, shift is applied to spatial edges in  $\Sigma_{l+1}$ , so the redundant equations are associated with the brace edges lying below the 3 cube-aligned vertex generator legs on  $\Sigma_{l+1}$ .

The Sorkin evolution scheme is, by construction, a partially constrained algorithm, since the redundant equations associated with shift edges at A- and C-type vertices are second order evolution-type equations, whereas at B- and D-type vertices we discard first order constraint-type equations. For simplicity we shall refer to the redundant shift equations at each vertex as the “Momentum constraints”, although they are in fact a mixture of first-order and second-order equations.

The evolution of an axisymmetric Kasner cosmology (with Kasner exponents  $p_1 = p_2 = 2/3, p_3 = -1/3$ ) is shown in figure 3, and figure 4 shows the evolution of an expanding flat space solution, corresponding to the Kasner exponents  $p_1 = p_2 = 0, p_3 = 1$ . Both runs cover a ten-fold increase in the three-volume. It can be seen that the fractional error in the three-volume remains small throughout the evolution. The fractional volume discrepancy is defined as

$$\frac{\Delta V}{V} = 1 - \frac{1}{V_0 t} \sum_{3V} V_i, \quad (15)$$

and the summation is over all tetrahedra on a  $t = \text{constant}$  surface.

Also apparent, particularly in the axisymmetric Kasner solution in figure 3, are high frequency oscillations (typical wavelengths of a few timesteps), which decrease in magnitude as the evolution proceeds. It was pointed out to us by R. Matzner that gravitational waves in a Kasner background would evolve with such a behaviour [30, 31]. We believe we are seeing a grid resolution limit effect reminiscent of such waves; however, in our case they are not fully resolvable. The oscillations are controllable, with magnitudes varying as  $l^2$  and wavelengths reducing as  $l$ , where  $l$  is a typical edge length on the lattice. The presence of these relatively high frequency, low amplitude waves does not appear to cause any instabilities, and it is apparent from figures 3 and 4 that the waves gradually die out as the lattice evolves.

The evolution of the three different classes of spatial cube-aligned edge are shown in figures 3c and 4c, and are found to closely match the expected Kasner evolution. In both figures the  $l_x$  and  $l_y$  edges lie atop one another. The standard deviation of the spatial edge  $l_z$ , shown in part d of the figures, increases gradually throughout the evolution. It reaches a few parts in  $10^{-10}$  after ten thousand timesteps for the axisymmetric Kasner solution, and remains below  $10^{-10}$  in the expanding flat spacetime of figure 4.

We now consider the convergence properties of the simplicial cosmological solution. Due to the global topology and homogeneity of the solution, we are able to examine convergence by reducing the typical scale length of the lattice, whilst keeping the number

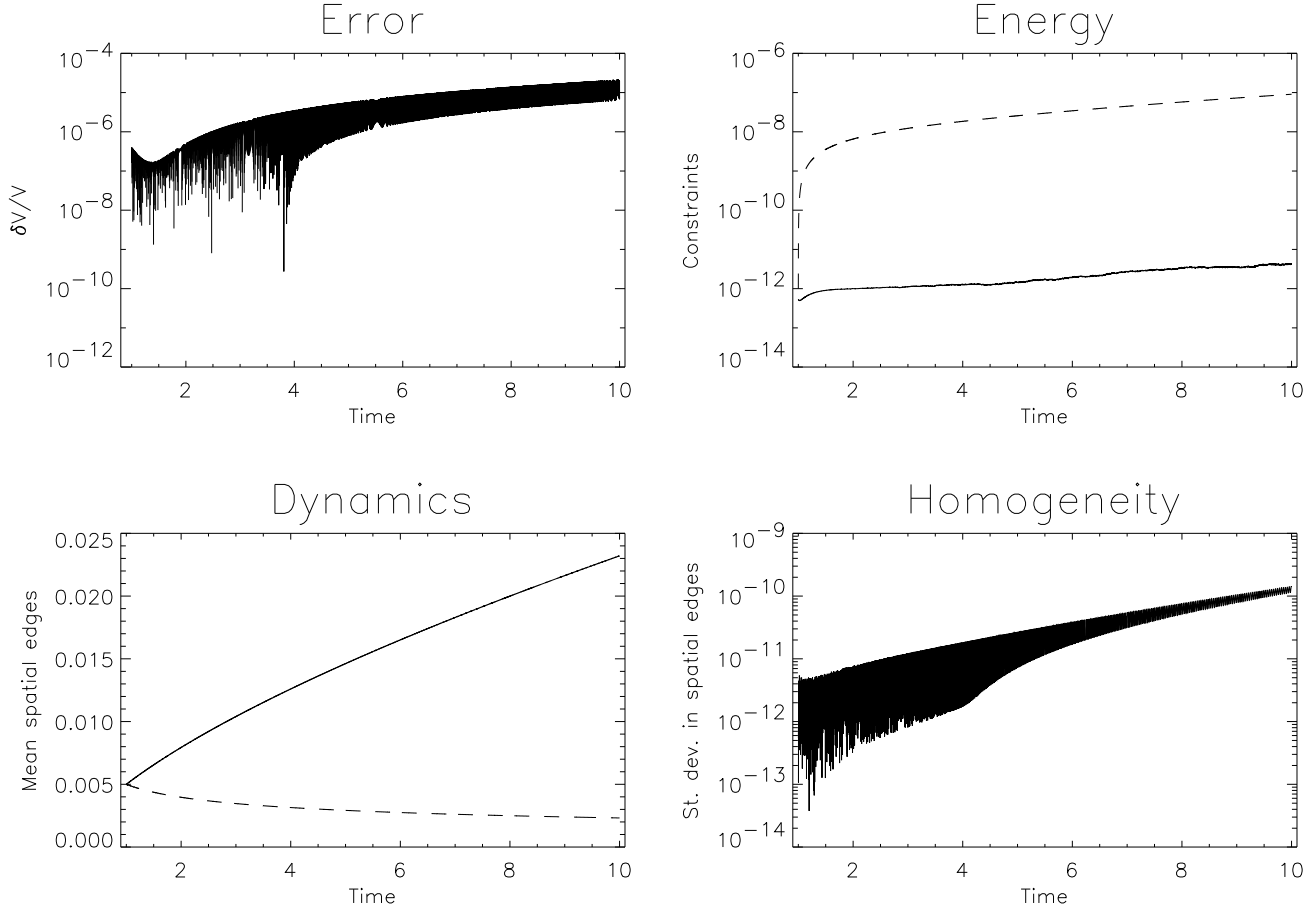


**Figure 3.** The axisymmetric simplicial Kasner solution with exponents  $(2/3, 2/3, -1/3)$ . The scale lengths are taken to be  $\Delta x = \Delta y = \Delta z = 0.005$ , and  $\Delta t = 0.001$ . a) The fractional error in the spatial 3-volume of the newly-evolved spacelike hypersurface is plotted against the proper time measured along timelike edges in the lattice. The error represents the fractional difference in the simplicial 3-volume from the expected linear growth rate. b) Growth of the Hamiltonian ( $--$ ) and Momentum ( $-$ ) constraints with time. c) Mean value of the spatial legs  $l_x$  ( $-$ ) and  $l_z$  ( $--$ ) against time. The legs display the expected power law behaviour, with the  $l_y$  leg being identical to  $l_x$  throughout the evolution. d) Standard deviation of the spatial leg  $l_z$  from mean. The other spatial legs  $l_x$ ,  $l_y$ , and  $l_d$  behave similarly.

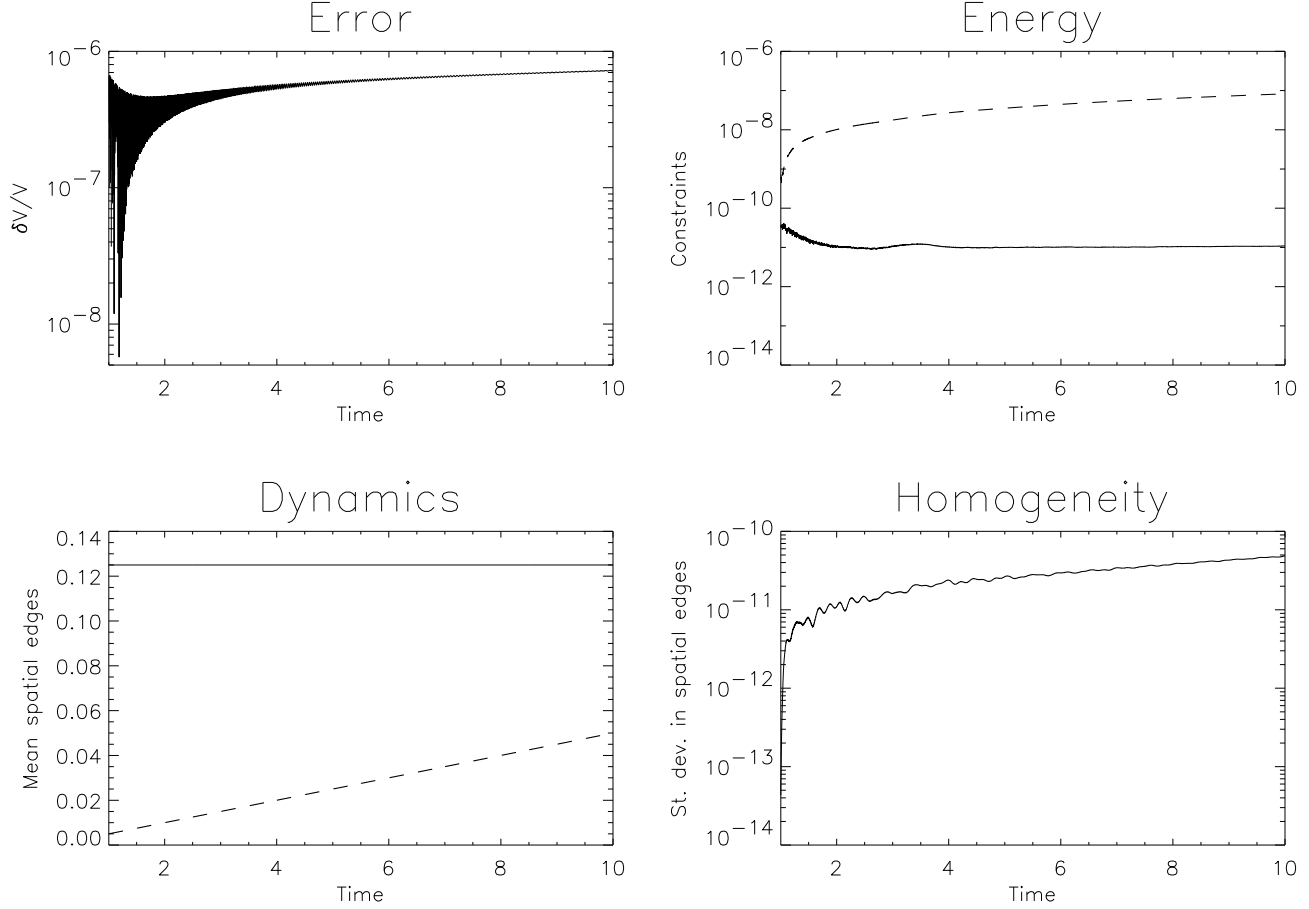


**Figure 4.** The flat Kasner solution, with exponents  $(0,0,1)$ . The lattice maintains homogeneity to a very high degree, with the standard deviation remaining below the limit of numerical accuracy (approximately  $1 \times 10^{-10}$ ). The spatial and temporal scales are  $\Delta x = \Delta y = 0.125$ ,  $\Delta z = 0.005$ , and  $\Delta t = 0.002$ . The same quantities are plotted as in the non-flat axisymmetric case shown in figure 3.

of vertices fixed. This is equivalent to looking at a smaller region of the total manifold. For the remainder of this section we introduce the scale parameter  $\delta$ , defined such that

$$\Delta x = \Delta y = \Delta z = \frac{\delta}{4} \quad \text{and} \quad \Delta t = 0.05 \times \delta, \quad (16)$$

which ensures that the Courant condition remains satisfied, and the total volume of the initial base three-geometry is  $\delta^3$ .

There are several important convergence issues that must be examined in Regge calculus, and our fully simplicial  $(3+1)$  calculation provides an excellent opportunity to do so for a specific application. The first, and most important issue to address

is the convergence of simplicial solutions to the corresponding solutions of Einstein's equations. The second issue is the consistency of the Regge equations. That is, as the typical lattice length scale is reduced, do the redundant Regge equations also converge? This latter question is related to the simplicial Bianchi identities, and the conservation of energy momentum. We find convergence in all solutions and equations.

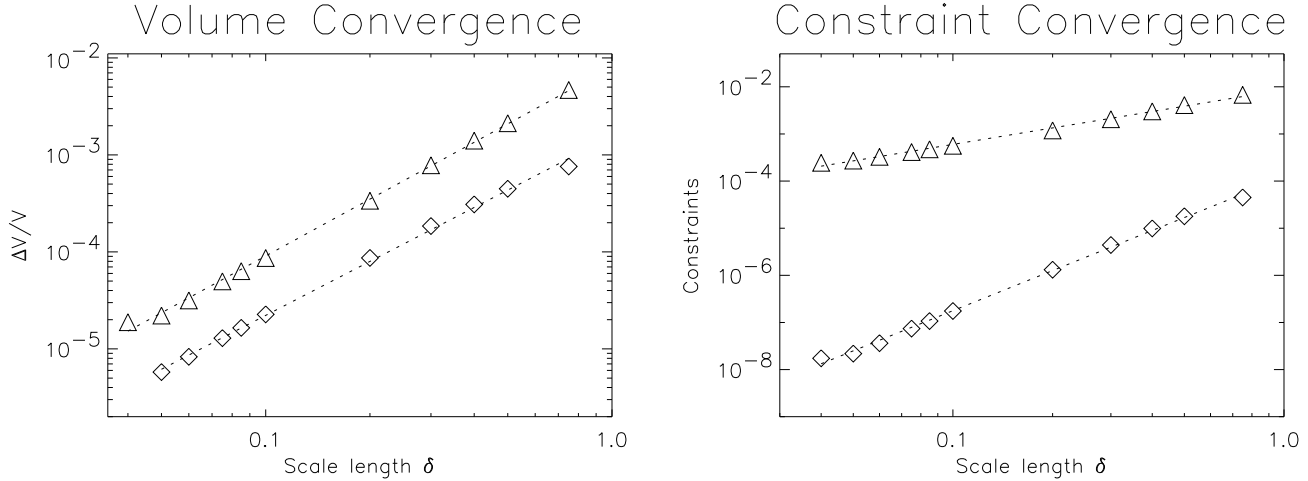


**Figure 5.** Convergence estimates for the axisymmetric Kasner model shown in figure 3. a) The average value of the fractional volume discrepancy, equation (15) evaluated at  $t = 8$ , is plotted against the overall scale parameter  $\delta$  ( $\Delta$ -points). The convergence in the diagonal spatial legs ( $\diamond$ -type points), also evaluated at  $t = 8$ , is shown. Both the error in the volume and the diagonal legs scales as the second power of  $\delta$ . This confirms, for the axisymmetric simplicial Kasner cosmology at least, that the solution of the Regge equations is a second order accurate approximation to the continuum solution. All other spatial legs were found to converge as second order in the scale length. b) The average magnitude of the constraint equations, evaluated at  $t = 8$ , plotted against the lattice scale length  $\delta$ . The momentum constraints ( $\diamond$ -type points) display slightly better than second order convergence. The Hamiltonian constraints ( $\Delta$ -type) scale linearly with  $\delta$ .

The error in lattice edge lengths compared to corresponding geodesic segments in the continuum was examined, together with the fractional difference of the simplicial three volume from linear expansion displayed by the continuum. The fractional volume discrepancy, (15), was evaluated at  $t = 8$ , although due to the fluctuations apparent in figure 3, the values were averaged over several periods of the oscillation. The results are shown in figure 5.

Figure 5 also shows that the diagonal spatial edges converge to the continuum solution second order in the typical lattice scale length. All other spatial edges were

found to converge at the same rate. This indicates that the simplicial Kasner solution converges to the continuum solution as the second power of the lattice spacing  $\delta$ .

Recent work has cast doubt over the convergence of Regge calculus to the continuum [5, 6, 7]. The calculations of Brewin applied continuum geodesic lengths directly to the lattice, and evaluated the Regge equations on the resulting simplicial spacetime. Numerical convergence tests indicated that the Regge equations failed to converge as the scale length of the lattice was decreased. We have shown explicitly, for one of the cases studied by Brewin, that solutions of the Regge equations converge to the corresponding solution of the continuum Einstein equations.

Figure 5 also displays the convergence of the redundant Regge equations as the lattice is refined. The standard deviation of the Momentum constraints, a combination of both evolution and true constraint-type equations, is shown to converge as at least the second power of  $\delta$ . The Hamiltonian constraint shows linear convergence. The convergence of the equations is consistent with the Regge Bianchi identities, and the existence of diffeomorphism freedom in Regge calculus.

The convergence analysis shows that for the Kasner cosmological model, Regge calculus is a second order discretization of Einstein's theory of gravity.

## 7. From BKL to Geons; future directions in Regge calculus

We have successfully performed the first fully  $(3+1)$ -dimensional calculation in Regge calculus, without the imposition of symmetry conditions. In the process we applied a novel 2-surface initial value formalism to the lattice, demonstrated the gauge freedom implied by the simplicial form of the contracted Bianchi identities, and showed explicitly that the solution of the Regge equations converges to its continuum counterpart.

The simplicial Kasner solution was found to agree well with the analytic solution, and maintains a remarkable degree of homogeneity throughout the evolution. Convergence analysis showed that all edge lengths converge to their continuum values as the second power of the typical lattice length scale, countering recent doubts over the convergence of Regge calculus to general relativity. The Regge constraint equations, arising from simplicial gauge freedoms, were also found to converge to zero as the lattice was refined. This demonstrates explicitly the existence of gauge freedom in the lattice, the simplicial counterpart of coordinate freedom in continuum general relativity.

Three issues direct our research in the immediate future. First is an analytic formulation of the convergence properties of the Regge equations, and their solutions. Secondly, we wish to provide an  $S^3 \times R^1$  benchmark of our code, based on a Taub-like cosmology. Finally, we are investigating planar numerical perturbations [29] of the Kasner cosmology, in order to analyze gravity wave propagation in our simplicial spacetime geometry.

In the longer term we intend to address three issues using Regge calculus. The first is related to the wiring of matter terms to the lattice geometry. We cannot think of a better approach than to utilize the Cartan analysis [4] described in section 3. With a formulation of matter in Regge calculus, we can begin to study the generic properties of collapse in inhomogeneous cosmologies. At both early and late stages in cosmological expansion, the effective gravity wave energy density dominates the contributions from matter and radiation fields. For this reason we wish to investigate geon states [32, 8] of the gravitational field [12]. We believe that these goals provide a clear direction for the future development of Regge calculus.

## Acknowledgments

We wish to thank John A. Wheeler for his continued encouragement to tackle this problem. We are also indebted to Leo Brewin, Ben Bromley, Arkady Kheyfets, Pablo Laguna, Richard Matzner and Ruth Williams for many stimulating discussions on this and related topics. We wish to acknowledge support for this work from an LDRD grant from Los Alamos National Laboratory, and the Sir James McNeill Foundation.

## References

- [1] T. Regge, *Nuovo Cimento* , **19**, 558 (1961).
- [2] R. M. Williams and P. A. Tuckey, *Class. Quantum Grav.* , **9**, 1409–22 (1992).
- [3] J. W. Barrett, M. Galassi, W. A. Miller, R. D. Sorkin, P. A. Tuckey and R. M. Williams, *Int. J. Theor. Phys.*, **36**, 815–39 (1997).
- [4] W.A. Miller, *Found. Phys.*, **16**, 143 (1986).
- [5] L. C. Brewin, gr-qc/9502043.
- [6] M. A. Miller, *Class. Quantum Grav.* , **12**, 3037 (1995).
- [7] M. P. Reisenberger, *Class. Quantum Grav.* , **14**, 1753–70 (1997).
- [8] J. A. Wheeler, in *Relativity, Groups and Topology*, ed. C. DeWitt and B. DeWitt (Blackie and Son Ltd., 1964)
- [9] C. W. Misner, K. S. Thorne and J.A. Wheeler, *Gravitation*, W.H. Freeman, San Francisco, 1973.
- [10] W. A. Miller, *Class. Quantum Grav.* , **14**, L199–L204 (1997).
- [11] A. Kheyfets, N. J. LaFave, and W. A. Miller, *Phys. Rev.* , **D41**, 3637 (1990).
- [12] V. A. Belinsky, I. M. Khalatnikov and E. M. Lifshitz, *Adv. Phys.*, **19**, 252 (1970).
- [13] W. A. Miller in *Dynamical spacetimes and Numerical Relativity*, ed. J. Centrella (Cambridge Univ. Press, 1986).
- [14] M. Miller, Ph.D Thesis, University of New York (Syracuse).
- [15] R. D. Sorkin, *Phys. Rev.* , **D12**, 385–96 (1975).
- [16] P. A. Tuckey, *Class. Quantum Grav.* , **10**, L109–13 (1992).
- [17] C. Y. Wong, *J. Math. Phys.* , **12**, 70–8 (1971).
- [18] P. A. Collins and R. M. Williams, *Phys. Rev.* , **D5**, 1908–12 (1972).
- [19] P. A. Collins and R. M. Williams, *Phys. Rev.* , **D7**, 965–71 (1973).

- [20] L. C. Brewin, *Class. Quantum Grav.* , **4**, 899–928 (1987).
- [21] R. M. Williams, *Gen. Rel. Grav.*, **17**, 559–71 (1985).
- [22] M. R. Dubal, *Class. Quantum Grav.* , **6**, 141–55 (1971).
- [23] A. P. Gentle, in *Proc. First Australasian Conf. on Gen. Rel. Grav.*, ed. D. L. Wiltshire (Uni. Adelaide, 1996).
- [24] A. P. Gentle, A. Kheyfets, and W. A. Miller, (in preparation).
- [25] J. A. Wheeler, *Int. J. Mod. Phys.*, **A3**, 2207–46 (1988).
- [26] E. P. Belasco and H. C. Ohanian, *J. Math. Phys.* , **10**, 1503–07 (1969).
- [27] S. M. Lewis, *Phys. Rev.* , **D25**, 307 (1982).
- [28] A. P. Gentle, unpublished (1995).
- [29] J. Centrella, in *Dynamical spacetimes and Numerical Relativity*, ed. J. Centrella (Cambridge Univ. Press, 1986).
- [30] R. A. Matzner, Private communication, May 1997.
- [31] T. E. Perko, R. A. Matzner and L. C. Shepley, *Phys. Rev.* , **D6**, 969 (1972).
- [32] J. A. Wheeler, *Phys. Rev.* , **97**, 511 (1955).